International Journal of Thermophysics, Vol. 25, No. 5, September 2004 (© 2004)

Normal Spectral Emissivity at a Wavelength of 684.5 nm and Thermophysical Properties of Solid and Liquid Molybdenum[1]

C. Cagran,[2] B. Wilthan,[2] and G. Pottlacher[2,3]

Polarimetric emissivity measurements adapted for a rapid pulse heating setup and recent results of normal spectral emissivity at 684.5 nm for molybdenum at melting and in the liquid phase are presented. Also reported is a complete set of thermophysical data (specific enthalpy, isobaric heat capacity, electrical resistivity, thermal conductivity, and thermal diffusivity) for molybdenum for both solid and liquid states. The results for all mentioned thermophysical properties are discussed and furthermore compared to literature values. The normal spectral emissivity and the electrical resistivity of molybdenum show opposite trends in the liquid phase, leading to the conclusion that a prediction of normal spectral emissivity at the given wavelength of 684.5 nm based on the Hagen–Rubens-relation and electrical resistivity measurements is not applicable.

KEY WORDS: ellipsometry; Hagen–Rubens-relation; molybdenum; normal spectral emissivity; pulse-heating; thermal conductivity; thermal diffusivity; thermophysical properties.

1. INTRODUCTION

Thermophysical properties of pure metals and alloys have been widely studied to support, on one hand, the metal working industry by using

[1]Paper submitted to the Fifteenth Symposium on Thermophysical Properties, June 22–27, 2003, Boulder, Colorado, U.S.A.

[2]Institute for Experimental Physics, Graz University of Technology, Petersgasse 16, A-8010 Graz, Austria.

[3]To whom correspondence should be addressed. E-mail: pottlacher@tugraz.at

0195-928X/04/0900-1551/0

them as input for computer simulations, and on the other hand, for a better scientific understanding of different physical processes. Casting simulations have become a very powerful and almost essential tool in process design and preproduction modeling of new parts, i.e., for the automobile industry. Therefore, a need for ever more and more accurate thermophysical data arises for known materials, and there is always a strong need for data for new materials such as Ti-aluminides or magnesium-based alloys. Our research group has been measuring such thermophysical properties for a long period of time and has always tried to enhance data for already measured materials (even our own measurements) as well as to have a focus on new alloys like Ti-Al-Nb-B [1] and, up to now, unspecified metals.

The data presented in this paper belong to the first category, since thermophysical properties of solid and liquid molybdenum have already been published [2], but are now expanded to cover thermal conductivity and thermal diffusivity, which we have not published before. The latest and probably most innovative addition in our range of measured properties is the normal spectral emissivity at a wavelength of 684.5 nm, because its determination into the liquid state has always been a difficult task. Therefore, literature data are not easily available and a need exists for those measurements, in particular for computer simulations.

The thermophysical properties presented in this paper have been determined using a resistive pulse-heating technique, which has been demonstrated to produce reproducible and accurate measurements from the solid state (some hundred kelvin below the melting point) up into the liquid phase. Additionally, we have incorporated DSC (differential-scanning calorimetry) measurements into our set of data by obtaining enthalpy versus temperature results starting from almost room temperature ($\sim$ 500 K) up to a maximum temperature of about 1500 K. The values obtained with this technique can not only be used to supplement our enthalpy and heat capacity measurements but also can be used to expand our temperature range down into the solid state [3].

Normal spectral emissivity measurements have been performed with a laser polarimetry technique (μs-DOAP [division-of-amplitude photopolarimeter]), which is one of the few available techniques able to obtain emissivity data in the liquid state under pulse-heating conditions. Due to the use of a laser as the light source, our emissivity measurements are limited to the initial wavelength (684.5 nm) of the laser. Although it would be generally possible to change the measurement wavelength of the DOAP by using different lasers and optical elements for the detection, this modification would be expensive and time-consuming.

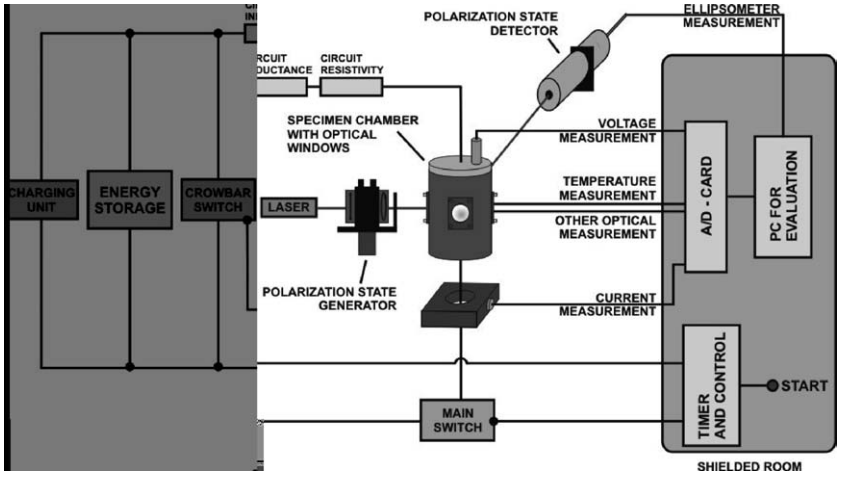

Fig. 1. Schematic diagram of the pulse-heating setup including the DOAP experiment.

2. EXPERIMENT SETUP AND DATA REDUCTION

2.1. Pulse-Heating Setup

The basic principle behind this technique is to pass a large current pulse through a wire-shaped specimen (typically 0.5 mm diameter), which causes a rapid increase in the temperature due to the resistance of the material under investigation. In our case, we obtain heating rates of about $10^8\,\mathrm{K\cdot s^{-1}}$, which results in an average experimental duration of about 30–60 μs per single measurement. See Ref. 4 for more details of the pulse-heating system. (A schematic overview of the experiment is presented in Fig. 1.) The time(t)-dependent quantities measured during such a pulse-heating experiment consist of the current, $I(t)$, through the specimen wire measured with a calibrated induction coil (Pearson Electronics, Inc.), the voltage drop, $U(t)$, across the specimen determined by means of two knife-edge probes, and the surface radiation of the wire, $J(t)$, obtained by means of a fast optical pyrometer. Starting with these three measured quantities, all other thermophysical data can be calculated as shown in Fig. 2.

2.1.1. Temperature

The temperature is calculated based on the pyrometrically determined surface radiation of the sample by using Planck's radiation law. To minimize the uncertainty arising from the wavelength in Planck's law, narrow interference (IF) filters (in our case: 37 nm FWHM at a center wavelength

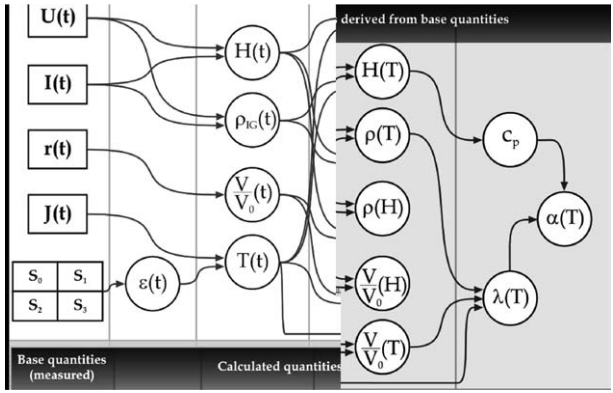

Fig. 2. Schematic drawing of directly measured and calculated quantities. U: voltage; I: current; r: specimen radius; J: surface radiation; t: time; $s_0 - s_3$: Stokes parameters; ε : emissivity; H: enthalpy; ρ_{IG}: electrical resistivity (initial geometry); V/V_0: volume expansion; T: temperature; ρ: electrical resistivity (referred to in text as ρ_{Vol}); c_p: specific heat capacity; a: thermal diffusivity; and λ : thermal conductivity.

of 650 nm) must be used in the pyrometers. Therefore, each pyrometer is only designed for a specific temperature range (based on the IF-filter and the photodiode used) and is generally not sensitive to temperatures below 1200–1500 K [3]. The radiation temperature of the sample at the effective wavelength λ of the pyrometer, T_{Rad}, is obtained using the voltage output S of a calibrated pyrometer as

$$T_{Rad} = \frac{c_2}{\lambda \ln\left(\frac{K}{S} + 1\right)}, \tag{1}$$

where K is the calibration factor of the pyrometer system and c_2 is the second radiation constant. The true sample temperature T can be obtained with the help of Planck's law by the following equation:

$$T = \frac{c_2}{\lambda} \frac{1}{\ln\left[\varepsilon\left(e^{\frac{c_2}{\lambda T_{Rad}}} - 1\right) + 1\right]}, \tag{2}$$

where ε is the normal spectral emissivity at the wavelength λ. As one can see, the actual value of the normal spectral emissivity at the wavelength of the pyrometer is needed for this procedure. If the temperature dependence of the normal spectral emissivity is not explicitly known, a constant emissivity value in the liquid phase has to be assumed for temperature evaluations, see, i.e., Ref. 5.

2.1.2. Enthalpy and Resistivity

The voltage used in the calculations is the measured value corrected for inductive contributions. The specific enthalpy, $H(t)$, is calculated from $U(t)$ and $I(t)$, starting at room temperature (although the temperature measurement starts at higher temperatures):

$$H(t) = \frac{1}{m} \int I(t)\, U(t)\, dt, \tag{3}$$

where m is the mass of the sample (between the voltage probes).
The electrical resistivity ρ_{IG} for the initial geometry may be calculated by

$$\rho_{\mathrm{IG}}(t) = \frac{U(t)\pi r^2}{I(t)\ell}, \tag{4}$$

where r is the sample radius at room temperature and ℓ is the length of the specimen. For further evaluation the change in volume has to be taken into consideration for the electrical resistivity, ρ_{Vol}, as the specimen wire expands during the heating process. ρ_{Vol} is basically obtained by multiplying ρ_{IG} by $V/V_0(T)$.

2.1.3. Thermal Conductivity and Thermal Diffusivity

The thermal conductivity λ may be estimated from the temperature-dependent electrical resistivity ρ_{Vol} by using the Wiedemann–Franz - law (W-F-L) in its well known form:

$$\lambda(T) = \frac{LT}{\rho_{\mathrm{Vol}}(T)}, \tag{5}$$

where T is the temperature and L is the Lorentz number, $L = 2.45 \times 10^{-8}\,\mathrm{V^2 \cdot K^{-2}}$, assuming that the Lorentz number is invariant in the region of interest. Based on a knowledge of the thermal conductivity, the thermal diffusivity a may be estimated from

$$a(T) = \frac{\lambda(T)}{c_p(T)d(T)}, \tag{6}$$

where c_p is the isobaric heat capacity and $d(T)$ is the density.

2.2. Differential Scanning Calorimetry (DSC)

The DSC is primarily used to measure the temperature dependence of the specific heat capacity (under constant ambient pressure) $c_p(T)$. By integrating the specific heat capacity values, the enthalpy can be directly

calculated (with reference to the value H_{298} at room temperature). Therefore, $H(T)$ for the solid state starting at the DSC onset temperature at about 500–1500 K can be obtained. This dependence can be used to assign a temperature scale to the electrical measured quantities during a pulse-heating experiment (i.e., enthalpy, resistivity) below the pyrometer onset temperature. More details are given in Ref. 3.

2.3. μs-Division-Of-Amplitude Photopolarimeter (μs-DOAP)

The normal spectral emissivity at 684.5 nm is measured by using a so-called division-of-amplitude photopolarimeter. The DOAP uses an ellipsometric measurement approach but without any rotating devices with regard to the time scale used for a pulse-heating experiment. This technique has first been described by Azzam [6] and uses the Stokes formalism for polarized light. Basically, a polarized laser beam is focused on the surface of the sample wire and the change in polarization of the reflected beam is analyzed. For more details see Refs. 7 and 8.

The detected signals are split into four intensities (hence, the name division-of-amplitude) from which the complex refractive index n and the extinction coefficient κ for the sample material are calculated. These two quantities are used to determine the normal spectral reflectivity R at the given wavelength by the following equation:

$$R = \frac{(n-n_0)^2+\kappa^2}{(n+n_0)^2+\kappa^2}, \tag{7}$$

where n_0 is the refractive index of the ambient medium. Finally, the normal spectral emissivity $\varepsilon(\lambda)$ can be calculated for opaque materials by using Kirchoff's law:

$$\varepsilon(\lambda) = 1 - R(\lambda). \tag{8}$$

Further details on μs-DOAP emissivity measurements are given in Ref. 8.

3. MEASUREMENTS AND RESULTS

All measurements in this study have been performed on wire-shaped molybdenum specimens with a diameter $\varnothing = 0.5$ mm and an average length of about 70 mm total (50 mm active length). The material was purchased from Goodfellow Cambridge Limited with the following specifications:

purity: 99.95%, hardness: annealed. Additionally, for emissivity measurements a molybdenum wire from Plansee (purity: n/a, surface: electropolished) was used for comparisons.

3.1. Results

All results given within this section represent averages of different measurements. For thermophysical properties, six independent measurements (the deviation between each of the single experiments was better than 1%) have been used to obtain the averaged results. For the normal spectral emissivity eight independent measurements have been used due to weaker signal-to-noise levels. Following Ref. 9, a melting temperature of $T_m = 2895\,K$ was used for all evaluations.

3.1.1. Normal Spectral Emissivity

Figure 3 shows the normal spectral emissivity of molybdenum in the liquid state. The linear least-squares fit for the liquid phase is

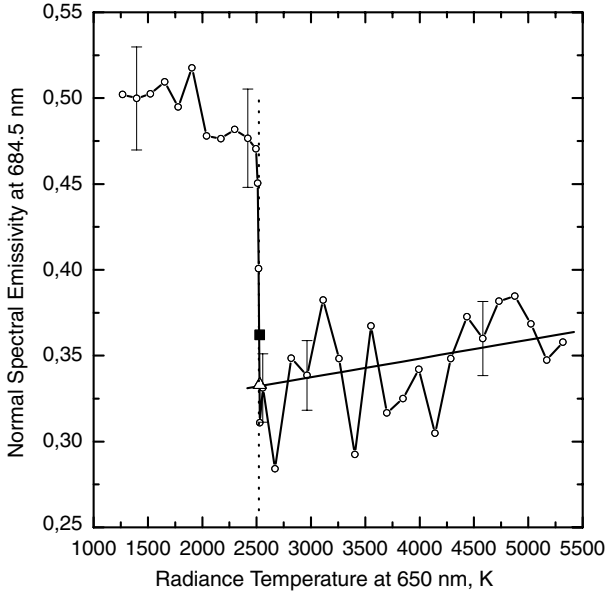

Fig. 3. Normal spectral emissivity of molybdenum at 684.5 nm as a function of radiance temperature at 650 nm. Open circles: emissivity (average of eight measurements); vertical dotted line: radiance temperature at melting (2520 K); open triangle: literature value of Ref. 10; filled square: reference value taken from Ref. 11.

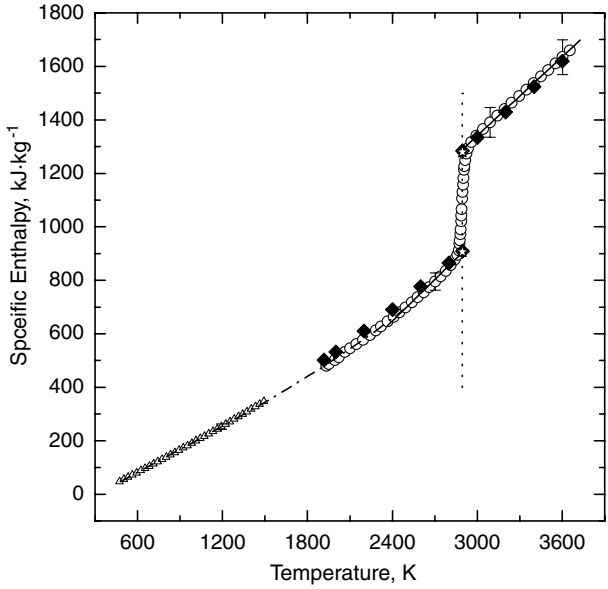

Fig. 4. Specific enthalpy of molybdenum as a function of temperature. Open circles: values obtained by pulse-heating; open triangles: values obtained with DSC; solid lines: linear least-squares fits to the end of the solid and the begin of the liquid phase; dashed line: fit to the temperature region from 400 to 2460 K; vertically dotted line: melting temperature; filled squares: literature values from Ref. 12; open stars: values from Ref. 13.

$$\varepsilon(T_{\mathrm{rad}}) = 0.3047 + 1.0902 \times 10^{-5} T_{\mathrm{rad}}, \qquad 2520\,\mathrm{K} < T_{\mathrm{rad}} < 5000\,\mathrm{K} \tag{9}$$

where T_{rad} is the radiance temperature at $\lambda = 650\,\mathrm{nm}$. At the end of melting, the emissivity is $\varepsilon(T_{\mathrm{rad,m}}) = 0.332$.

3.1.2. Enthalpy

Figure 4 presents the specific enthalpy obtained with the pulse-heating system as well as with the DSC. The fit for the solid state (combination of DSC and pulse-heating data; 3rd order) and the linear (least-squares) fit for the high-temperature region of the solid state are (H in $\mathrm{kJ \cdot kg^{-1}}$)

$$H_{\mathrm{s}}(T) = -98.7046 + 0.3183T - 3.8103 \times 10^{-5} T^2 + 1.5336 \times 10^{-8} T^3 \qquad 480\,\mathrm{K} < T < 2480\,\mathrm{K}, \tag{10}$$

$$H_{\mathrm{s}}(T) = -594.6586 + 0.5177T, \quad 2480\,\mathrm{K} < T < 2895\,\mathrm{K}, \tag{11}$$

$$H_l(T) = -133.7498 + 0.4916T, \quad 2895\,\mathrm{K} < T < 3600\,\mathrm{K}, \tag{12}$$

for the liquid state. For the above fits as well as for all further fits within this study, the subscripts are as follows. s: solid, l: liquid. At melting, $H_s(T_m) = 904.6\,\mathrm{kJ{\cdot}kg^{-1}}$ and $H_l(T_m) = 1289.9\,\mathrm{kJ{\cdot}kg^{-1}}$, yielding a heat of fusion of $\Delta H = 385.3\,\mathrm{kJ{\cdot}kg^{-1}}$. The entropy of fusion calculated by $\Delta S = \Delta H/T_m$ is $\Delta S = 133.05\,\mathrm{J{\cdot}kg^{-1}{\cdot}K^{-1}}$.

The values for the specific heat capacity are obtained from the slopes of the linear fits above. As is well known and confirmed by various measurements [14–16], the isobaric heat capacity c_p increases significantly in the solid state just before melting. Based on the slope of the enthalpy measurements performed in this study, only a constant heat capacity can be obtained for the solid and liquid states. Therefore, the c_p value for the solid state represents the estimated value at the onset of melting only and cannot be expected to be representativ e for a larger temperature range.

At the onset of melting (T_m = 2895 K), a mean value of $c_{p,s} = 517.7\,\mathrm{J{\cdot}kg^{-1}{\cdot}K^{-1}}$ is obtained, and a constant value of $c_{p,l} = 491.6\,\mathrm{J{\cdot}kg^{-1}{\cdot}K^{-1}}$ was found for the liquid phase.

3.1.3. Electrical Resistivity

Results for the electrical resistivity based on the initial geometry as well as values taking into account the volume expansion are presented in Fig. 5. The volume expansion of pure molybdenum was taken from the literature for the solid state [17] and for the liquid state [12]. Note that the resistivity values are shown in the solid state starting from 500 K.

The fits for the electrical resistivity with the initial geometry (ρ_{IG} in $\mu\Omega{\cdot}$m) are

$$\rho_{IG,s}(T) = -0.0384 + 2.8436\times10^{-4}T - 1.0970\times10^{-8}T^2 + 3.6622\times10^{-12}T^3 \quad 400\,\mathrm{K} < T < 2895\,\mathrm{K}, \tag{13}$$

$$\rho_{IG,l}(T) = 0.9535 - 1.1498\times10^{-5}T, \quad 2895\,\mathrm{K} < T < 3600\,\mathrm{K}. \tag{14}$$

The resistivity at the onset of melting is $\rho_{IG,s}(T_m) = 0.782\ \mu\Omega{\cdot}$m, and $\rho_{IG,l}(T_m) = 0.910\,\mu\Omega{\cdot}$m at the end of melting. Therefore, we obtain an increase in resistivity during melting of $\Delta\rho_{IG} = 0.128\,\mu\Omega{\cdot}$m.

The results taking into account the volume expansion (ρ_{Vol} in $\mu\Omega{\cdot}$m) are represented by the following fits:

$$\rho_{Vol,s}(T) = -0.0342 + 2.6770\times10^{-4}T + 6.7741\times10^{-9}T^2 + 9.6354\times10^{-13}T^3 \quad 400\,K < T < 2895\,K, \tag{15}$$

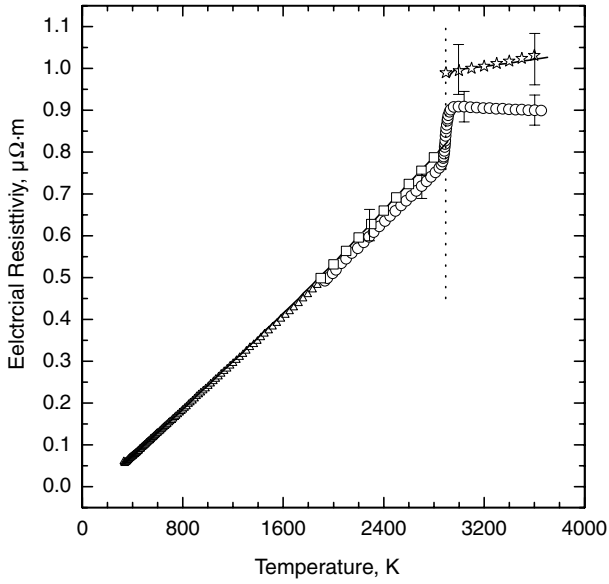

Fig. 5. Electrical resistivity (with initial geometry and with consideration of volume expansion) for molybdenum as a function of temperature. Open circles: data (initial geometry) from pulse-heating measurements; open triangles: pulse-heating data (initial geometry) incorporating the temperature scale from DSC experiments; solid line: volume corrected resistivity; vertically dotted line: melting temperature; open squares: literature values from Ref. 14; open stars: values from Ref. 12.

$$\rho_{\mathrm{Vol},1}(T) = 0.8483 + 4.8435 \times 10^{-5} T, \qquad 2895\,K < T < 3600\,K. \tag{16}$$

The resistivity at the onset of melting is $\rho_{\mathrm{Vol,s}}(T_{\mathrm{m}}) = 0.821\,\mu\Omega{\cdot}\mathrm{m}$, at the end of melting $\rho_{\mathrm{Vol},1}(T_{\mathrm{m}}) = 0.989\,\mu\Omega{\cdot}\mathrm{m}$. Therefore, we obtain an increase in the resistivity during melting of $\Delta\rho_{\mathrm{Vol}} = 0.168\,\mu\Omega{\cdot}\mathrm{m}$.

3.1.4. Thermal Conductivity and Thermal Diffusivity

Thermal conductivity (λ in $\mathrm{W{\cdot}K^{-1}{\cdot}m^{-1}}$) as shown in Fig. 6 in the solid and liquid phases is represented by the following fits:

$$\lambda_{\mathrm{s}}(T) = 111.1349 - 0.0126T + 1.4122 \times 10^{-6} T^2 \qquad 1500\,K < T < 2895\,K. \tag{17}$$

$$\lambda_l(T) = 11.4262 + 0.0208T, \qquad 2895\,\mathrm{K} < T < 3600\,\mathrm{K}. \tag{18}$$

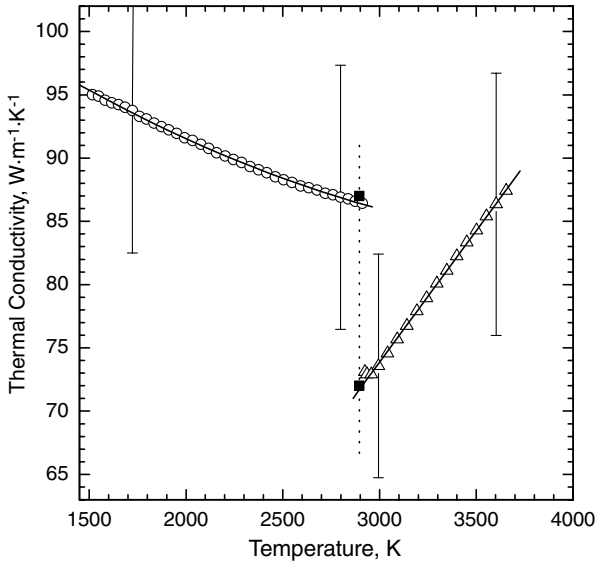

Fig. 6. Thermal conductivity of molybdenum as a function of temperature. Open circles: measured data for the solid state; open triangles: data for the liquid state; vertically dotted line: melting temperature; filled squares: reference values from Ref. 18.

The thermal conductivity at the onset of melting is $\lambda_s(T_m) = 86.4\,W{\cdot}K^{-1}{\cdot}m^{-1}$, and $\lambda_l(T_m) = 71.7\,W{\cdot}K^{-1}{\cdot}m^{-1}$ at the end of melting. Therefore, we obtain an increase in thermal conductivity during melting of $\Delta\lambda = 14.7\,W{\cdot}K^{-1}{\cdot}m^{-1}$.

The thermal diffusivity of molybdenum is not given in a separate figure, as its behavior is basically the same as for thermal conductivity in Fig. 6. The values for the thermal diffusivity (in $10^{-5}\,m^2{\cdot}s^{-1}$) are given by the following fits:

$$a_s(T) = 2.1212 \times 10^{-5} - 2.5475 \times 10^{-9}T + 4.2606 \times 10^{-13}T^2 \qquad 2500\,K < T < 2895\,K, \tag{19}$$

$$a_l(T) = 1.6210 \times 10^{-6} + 4.5065 \times 10^{-9}T, \qquad 2895\,K < T < 3600\,K. \tag{20}$$

The thermal diffusivity at the onset of melting is $a_s(T_m) = 1.74 \times 10^{-5}\,m^2{\cdot}s^{-1}$, and $a_l(T_m) = 1.47 \times 10^{-5}\,m^2{\cdot}s^{-1}$ at the end of melting. Thus, we obtain an increase in thermal diffusivity during melting of $\Delta\lambda = 0.27 \times 10^{-5}\,m^2{\cdot}s^{-1}$.

A summary of the measured thermophysical properties from this work and literature results is presented in Table I.

4. DISCUSSION

In the following section, specific details concerning each figure will be discussed further. Generally, it can be seen from Figs. 3–6 and Table I, that all of our measured values agree very well with the literature data.

4.1. Normal Spectral Emissivity

At the onset of melting, a strong decrease in emissivity can be seen in Fig. 3. In the liquid phase, the normal spectral emissivity of molybdenum at 684.5 nm shows an increase up to temperatures of 4500 K. This increase is in contradiction to the liquid-phase behavior of the electrical resistivity with initial geometry if one assumes the validity of the Hagen–Rubens-relation ($\varepsilon \propto f(\rho)$) at this wavelength. We have observed such an opposite behavior for different materials and thus strongly believe that the Hagen–Rubens-relation is not applicable for measurements at 684.5 nm. At the end of melting, a value of emissivity of $\varepsilon = 0.33$ is obtained, which seems to fit quite well with the available literature data, although the measurement wavelengths are not identical. Finally, we used molybdenum wires from two different manufacturers; although the values in the solid state were different due to varying surface structures, the specimens from both manufacturers did not only show the same behavior in the liquid phase but also gave the same value at melting.

4.2. Specific Enthalpy

We measured the enthalpy values in the range from 400 to 1500 K by DSC and from 1900 to 3600 K with the pulse-heating setup. Although the heating rates are completely different, both data sets agree quite well with each other, as can be seen in Fig. 4. This demonstrates that the pulse-heating experiment can be considered as quasi-static, as long as there are no solid-state phase transitions. As a result, a combined fit in the temperature range from 400 to 2460 K is given for molybdenum. The literature data [12, 13] agree quite well with our measured values.

4.3. Electrical Resistivity

Figure 5 depicts the electrical resistivity with initial geometry conditions as well as the electrical resistivity values considering volume

Table I. Summary of Properties of Molybdenum (specific enthalpy, H; heat of fusion, ΔH; specific heat capacity, c_p; specific electrical resistivity, ρ ; thermal conductivity, λ ; normal spectral emissivity, ε. Subscript s, solid; subscript l, liquid; T_m, melting temperature;*, extrapolated to T_m; +, values taken from Ref. 2)

Reference	H_s ($kJ \cdot kg^{-1}$)	H_l ($kJ \cdot kg^{-1}$)	ΔH ($kJ \cdot kg^{-1}$)	$c_{p,s}$ ($J \cdot kg^{-1} \cdot K^{-1}$)	$c_{p,l}$ ($J \cdot kg^{-1} \cdot K^{-1}$)	$\rho_{Vol,s}$ ($\mu\Omega \cdot m$)	$\rho_{Vol,l}$ ($\mu\Omega \cdot m$)	λ_s ($W \cdot K^{-1} \cdot m^{-1}$)	λ_l ($W \cdot K^{-1} \cdot m^{-1}$)	$\varepsilon(T_m)$
This work	904.6	1289.9	385.3	517.7	491.6	0.821	0.989	86.4	71.7	0.33 (684.5 nm)
[14]	–	–	–	523.3*	–	0.818*	–	–	–	–
[19]	–	–	379.4	–	–	–	–	–	–	–
[20]	–	–	363.1	–	357.4	–	–	–	–	–
[12]	909.2	1284.8	375.3	–	475	0.836	0.990	–	–	–
[13]	907	1280	373	–	–	0.801	0.955	–	–	–
[21]	888	1393	505	–	500	0.806	0.971	–	–	–
[22]	930.1	1296.5	339.4	545.5	357.4	–	–	–	–	–
[23, 2+]	910	1320	410	–	540	0.80	0.98	89+	72+	–
[18]	–	–	–	–	–	–	–	87	72	–
[24]	–	–	–	–	–	–	–	–	–	0.343 (657 nm)
[10]	–	–	–	–	–	–	–	–	–	0.335 (653 nm)
[15]	–	–	–	–	–	–	–	–	–	0.342 (633 nm)
[11]	–	–	–	–	–	–	–	–	–	0.345 (633 nm)

expansion. The temperatures obtained by DSC measurements of enthalpy have been used to extend the electrical resistivity results measured with the pulse-heating setup to lower temperature, $\sim$ 500 K. Although the volume expansion is taken from literature data [12,17], the resistivity values show excellent agreement with data reported by Refs. 12 and 14.

4.4. Thermal Conductivity and Thermal Diffusivity

By using the W-F-L, we calculated the thermal conductivity of molybdenum in the temperature range from 1500 to 3600 K. Comprehensive literature comparisons were not possible, since there are only few data for thermal conductivity available in this temperature range. Touloukian [25] presents reference data, but they are very dispersed over the entire range. As there is no recommendation given, the values are not used for comparison. Nevertheless, the National Physical Laboratory (NPL), United Kingdom gives recommended values for the thermal conductivity of molybdenum at the melting transition and our measured data show an almost exact match with them [18].

The thermal diffusivity is calculated based on our thermal conductivity values. A separate plot is not presented, since it shows almost the same behavior as for the thermal conductivity. Other than thermal conductivity, no literature data were available for comparisons in the temperature region of interest. The fit in the solid state ranges only from 2500 to 2895 K as the thermal diffusivity calculations use the specific heat capacity at the given temperature, which can only be obtained at the end of the solid state by pulse-heating measurements.

5. ESTIMATION OF UNCERTAINTIES

According to Ref. 26 uncertainties reported here are expanded relative uncertainties with a coverage factor of $k = 2$. Two lists of final evaluated sets of uncertainties are given, first for directly measured variables such as current, I, 2%, voltage drop, U, 2%, temperature, T, 4%, and mass, m, 2%. For the calculated thermophysical properties one obtains the following uncertainties: enthalpy, H, 4%; enthalpy of melting ΔH, 8%; specific heat capacity c_p, 8%; specific electrical resistivity with initial geometry, ρ_{IG}, 4%; resistivity considering volume expansion, ρ_{Vol}, 6%; thermal conductivity, λ, 12%; and thermal diffusivity, a, 16%.

An estimation of uncertainty for the normal spectral emissivity, ε, is performed by determining the signal-to-noise ratio of different individual measurements and by analyzing the reproducibility of different measurements. For investigations on liquid molybdenum the signal-to-noise ratio

of a single experiment does not exceed 6%. By averaging several different measurements to minimize the noise of the emissivity signals and applying a linear least-squares fit to the liquid-phase behavior of the normal spectral emissivity, the uncertainty can be reduced by up to a factor of 2, thus yielding an uncertainty of ±3%. By including the coverage factor of $k = 2$, one obtains an uncertainty for the normal spectral emissivity for liquid molybdenum of ±6%, respectively.

6. CONCLUSION

We have measured a complete set of thermophysical properties of molybdenum in the solid and liquid states. Our measurements are in excellent agreement with those appearing in the literature. In addition to the past studies on the thermophysical properties of molybdenum, we also present values for the thermal conductivity as well as the thermal diffusivity at the melting transition and in the liquid phase. Additionally, measurements of the normal spectral emissivity for liquid molybdenum at 684.5 nm are presented in the current work. As we discovered in previous measurements, the liquid phase behavior of the normal spectral emissivity at 684.5 nm can be categorized as (a) decreasing, (b) constant, or (c) increasing [27]. Molybdenum seamlessly fits into category (c) of this classification, as the normal spectral emissivity shows a slight increasing trend throughout the liquid phase. Furthermore, the results of the normal spectral emissivity and the electrical resistivity (with initial geometry) of liquid molybdenum show opposite behaviors. Thus, the Hagen–Rubens-relation is not applicable to predict the liquid-phase behavior of the emissivity at 684.5 nm with a knowledge of the electrical resistivity behavior with initial geometry.

Since the change in emissivity during the liquid phase is small, all measurements from other authors, without consideration of the actual behavior of emissivity, are not expected to differ significantly from values of this work.

ACKNOWLEDGMENT

This work has been supported by the *FWF*, "Fonds zur Foerderung der wissenschaftlichen Forschung", Grant P-15055.

REFERENCES

1. C. Cagran, B. Wilthan, G. Pottlacher, B. Roebuck, M. Wickins, and R. A. Harding, *Intermetallics* **11**:1327 (2003).

2. G. Pottlacher, *J. Non-Cryst. Solids* **250–252**:177 (1999).
3. B. Wilthan, C. Cagran, and G. Pottlacher, *Int. J. Thermophys*. **25**:1519(2004).
4. E. Kaschnitz, G. Pottlacher, and H. Jäger, *Int. J. Thermophys*. **13**:699 (1992).
5. G. R. Gathers, *Int. J. Thermophys*. **4:**149 (1983).
6. R. M. A. Azzam, *Opt. Acta* **29**:685 (1982).
7. A. Cezairliyan, S. Krishnan, and J. L. McClure, *Int. J. Thermophys*. **17**:1455 (1996).
8. A. Seifter, F. Sachsenhofer, and G. Pottlacher, *Int. J. Thermophys*. **23**:1267 (2002).
9. R. E. Bedford, G. Bonnier, H. Maas, and F. Pavese, *Metrologia* **33**:133 (1996).
10. A. P. Miiller and A. Cezairliyan, *Temperature—Its Measurement and Control in Science and Industry*, Vol. 6, J. F. Schooley, ed. (AIP, Melville, New York, 1992), p. 769.
11. T. Matsumoto, A. Cezairliyan, and D. Basak, *Int. J. Thermophys*. **20**:943 (1999).
12. R. S. Hixson and M. A. Winkler, *Int. J. Thermophys*. **13**:477 (1992).
13. J. W. Shaner, G. R. Gathers, and C. Minichino, *High. Temp. – High. Press*. **9**:331 (1977).
14. A. Cezairliyan, M- S. Morse. H. A. Berman, and C. W. Beckett, *J. Res. Nat. Bur. Stand. (U.S.)* **74A**:65 (1970).
15. A. Cezailriyan, S Krishnan, D. Basak, and J. L. McClure, *Int. J. Thermophys*. **19**:1267 (1998).
16. A. Cezairliyan, *Int. J. Thermophys*. **4**:159 (1983).
17. A. Goldsmith, T. E. Waterman, and H. J. Hirschorn, eds., *Handbook of Thermophysical Properties of Solid Materials*, Vol. 1—*Elements* (Pergamon Press, Oxford, 1961).
18. K. C. Mills, B. J. Monaghan, and B. J. Keene, *Thermal Conductivities of Liquid Metals—Part 1:Pure Metals*, NPL Report CMMT(A) 53 (1997).
19. J. L. McClure and A. Cezairliyan, *Int. J. Thermophys*. **11**:731 (1990).
20. J. A. Treverton and J. L. Margrave, *Proc. 5th Symp. Thermophys. Props*., C. F. Bonilla, ed. (ASME, New York, 1970), p. 489.
21. U. Seydel, W. Fucke, and H. Wadle, *Die Bestimmung Thermophysikalischer Daten flüssiger Metalle mit Schnellen Pulsaufheizexperimenten* (P. Mannhold, Düsseldorf, 1980).
22. R. Hultgren, P. D. Desai, D. T. Hawkins, M. Gleiser, K. K. Kelley, and D. D. Wagman, *Selected Values of the Thermodynamic Properties of the Elements*, American Society for Metals, UMI, Reprinted (1990).
23. G. Pottlacher, E. Kaschnitz, and H. Jäger, *J. Non-Cryst. Solids* **156–158**:374 (1993).
24. A. Cezairliyan and A. P. Miiller, *Int. J. Thermophys*. **14**:1109 (1993).
25. Y. S. Touloukian, R. W. Powell, C.Y. Ho, and P. G. Klemens, *Thermal Properties of Matter*—Vol. 1 (Plenum, New York, 1970).
26. Expression of the Uncertainty of Measurement in Calibration, EA-4/02. http://www.european-accreditation.org/pdf/EA-4-02ny.pdf
27. C. Cagran, C. Brunner, A. Seifter, and G. Pottlacher, *High Temp.-High. Press*. **34**:669 (2003).